PHYSICAL REVIEW B **74**, 134410 (2006)

Magnetoresistivity as a probe to the field-induced change of magnetic entropy in RAl_2 compounds (R=Pr,Nd,Tb,Dy,Ho,Er)

J. C. P. Campoy, E. J. R. Plaza, A. A. Coelho, and S. Gama
Instituto de Física "Gleb Wataghin," Universidade Estadual de Campinas, Caixa Postal 6165, 13083-970, Campinas, São Paulo, Brazil

(Received 10 October 2005; revised manuscript received 1 August 2006; published 13 October 2006)

The heat capacity $C_P(T)$ of the ferromagnetic compounds RAl_2 (R=Pr,Nd,Tb,Dy,Ho,Er) was measured at zero and applied magnetic field of 5 T in the temperature interval from 2 to 200 K. From these results are calculated the magnetic component of the entropy change, $-\Delta S_{mag}(T)=S(0,T)-S(H,T)$. From resistivity measurements, $\rho(H,T)$, from 2 to 300 K in the same compounds, we calculated the resistivity change due to the applied magnetic field, $-\Delta\rho_{mag}(T)=[\rho_{mag}(0,T)-\rho_{mag}(H,T)]$. The results are compared and we observed a similar dependence between $-\Delta\rho_{mag}(T)$ and $(T/T_C)^m\Delta S_{mag}(T)$ with $m=0$ for $T\geqslant T_C$ and $m=1$ for $T\leqslant T_C$. A simple model using a Hamiltonian considering molecular and crystalline electric fields, in a mean field approximation, is adopted for the calculus. Our results show that theory and experiment are in good agreement showing that the magnetoresistivity is a probe to the field-induced change of magnetic entropy in these compounds and can be extended to other materials. A model for the factor connecting both quantities, $-\Delta S_{mag}(T)$ and $-\Delta\rho_{mag}(T)$, is developed. This factor contains mainly the effective exchange integral which is related to Fermi energy that in turn is related to the electron effective mass.

DOI: 10.1103/PhysRevB.74.134410 PACS number(s): 75.30.Sg, 72.15.−v, 73.50.Jt, 74.70.Ad

INTRODUCTION

It is well known that the electrical resistivity ρ depends on the change in entropy of a magnetic system, caused, for instance, by external applied magnetic field and temperature changes.[1] We studied these dependences in the RAl_2 intermetallic compounds (R=rare earth) that crystallize in the cubic $MgCu_2$ type structure. In these compounds the rare earth elements are magnetic and aluminum is magnetically neutral. It is well accepted that the long range magnetic order in these compounds is due to the indirect spin exchange interaction between the localized magnetic moments on the rare earth atoms via the conduction electrons.[2] Additionally, the magnetic order as a function of the temperature will be changed by an external applied magnetic field, and it should be possible to characterize this change measuring the scattering of the conduction band electrons with and without field. So, the change of electrical resistivity, $-\Delta\rho_{mag}(T)=[\rho_{mag}(0,T)-\rho_{mag}(H,T)]$, will mainly reflect (limitations will be discussed) the magnetic state change of the system. The isothermal magnetic entropy change $-\Delta S_{mag}$, a measure of the magnetocaloric effect (MCE) in the RAl_2 compounds, also reflects the magnetic state change of the system and can be obtained indirectly from magnetic or heat capacity measurements. Strictly speaking, the MCE (the ability of a change on temperature of a material due to a variation of an external applied magnetic field) contains all entropy variations that can be induced by the change of the magnetic field but in general, the magnetic component, $-\Delta S_{mag}$, accounts for almost all the effect.[3] In certain materials some magnetoelastic contribution to the MCE can be observed but in the RAl_2 compounds this effect is negligible being $-\Delta S_{mag}\sim-\Delta S_{total}$.

In an early work, Potter[4] tried to connect the magnetoresistance and the magnetocaloric effect in some transition metals and alloys. He proposed the relation $C_P\Delta T_{mag}(T)=AT_C^n\Delta\rho_{mag}(T)/\rho_{mag}(0,T)$ between the adiabatic magnetocaloric potential, $\Delta T_{mag}(T)=-\int_0^H\left(\frac{T}{C_p}\frac{\partial M}{\partial T}\right)_{H'}dH'$, and $\Delta\rho_{mag}(T)$ around the transition, with A a constant and n being about 3. Afterwards, based on empirical results, Alexander *et al.*[5] suggested the relation $d\rho(T)/dT\propto C_P(T)$ which would be valid for the magnetic transition region in magnetoelectronic systems. From this relation one can derive the early one for $T>T_C$ because in this case $\rho_{mag}(0,T)$ is essentially a constant.

Studying the change of resistance of nickel in a magnetic field, Potter[6] found that $C_P\Delta T_{mag}(T)$ is almost proportional to $\Delta\rho_{mag}(T)/\rho_{mag}(0,T)$ in an extended range of temperatures, $T>0.75\ T_C$, showing that the connection between magnetoresistance and the magnetocaloric effect is not necessarily restricted to the transition region.

Because the magnetoresistivity contains a response to the degree of magnetic disorder, which can be adjusted by a magnetic field and measured by the magnetic entropy, it is possible to imagine a connection between the variations $\Delta\rho_{mag}$ and ΔS_{mag} due to the applied magnetic field. For systems in which we can extract adequately the field and temperature induced spin disorder resistivity, that connection can be tested. This condition is satisfied by many $R-X$ metallic systems and we choose the ferromagnetic RAl_2 series because of its importance as magnetocaloric materials and because it is well modeled in a mean field approximation.

In this work we compare measurements of both the magnetocaloric effect and magnetoresistivity for the series of compounds RAl_2 with R=Pr, Nd, Tb, Dy, Ho, and Er, for convenient experimental values of H=0 and 5 T. Both effects are theoretically described in a mean field model, and the comparison between the model and the experimental results is discussed. On the one hand, the proportionality factor connecting $-\Delta S_{mag}(T)$ and $-\Delta\rho_{\mathrm{mag}}(T)$ is obtained experimentally and from the model. On the other hand, our results suggest the relation $\Delta\rho_{mag}(T)\propto(T/T_C)^m\Delta S_{mag}(T)$ with $m=1$ for $T\leqslant T_C$ and $m=0$ for $T\geqslant T_C$.

THEORY

We consider the magnetic contribution for the electric resistivity, $\rho(H,T)$, in the easy axis of magnetization given by Ravishankar[7]

$$\rho_{mag}(H,T) = \rho^0_{mag} \times (\langle \hat{O}^1_{-1}\hat{O}^1_1\rangle + \langle \hat{O}^1_1\hat{O}^1_{-1}\rangle) \tag{1}$$

for the isotropic exchange scattering, where

$$\langle \hat{A}\hat{B}\rangle = \sum_{i,j} \frac{\exp(-\beta E_i)}{Z} \frac{\beta(E_i - E_j)}{1-\exp(-\beta(E_i - E_j))} \langle i|\hat{A}|j\rangle\langle j|\hat{B}|i\rangle.$$

In this equation the first factor is the Boltzmann population of the $4f$ rare earth ion state $|i\rangle$ and the second one is the integrated Fermi factor where Z is the partition function and $\beta = 1/k_B T$ (k_B is the Boltzmann constant). The $|i\rangle$ states are obtained from the single ion rare earth Hamiltonian

$$\hat{\mathrm{H}} = \hat{\mathrm{H}}_{CEF} + \hat{\mathrm{H}}_{mag}, \tag{2}$$

where

$$\hat{H}_{\mathrm{CEF}} = W\left[\frac{X}{F_4}(\hat{O}^0_4 + 5\hat{O}^4_4) + \frac{1-|X|}{F_6}(\hat{O}^0_6 - 21\hat{O}^4_6)\right], \tag{3}$$

and

$$\hat{H}_{mag} = -g\mu_B(H + \eta g\mu_B\langle \hat{O}^1_0\rangle)\hat{O}^1_0. \tag{4}$$

Equation (3) is the single-ion crystal electric field (CEF) Hamiltonian for cubic symmetry where W gives the CEF energy scale and X gives the relative contributions of the fourth and six degree in $\hat{O}^m_n$ Stevens' equivalent operators and F_4 and F_6 are characteristic constants of each rare earth ion. Equation (4) is the single-ion Zeeman and exchange terms where η is the exchange parameter, μ_B is the Bohr magneton, and g is the Landè factor. We obtained the normalized magnetoresistivity, $\{-\Delta\rho_{mag}\}$, directly from the operator part of Eq. (1) for the whole range of temperatures. On the other hand, it is well established that above T_C the first Born approximation gives a temperature independent term for the paramagnetic resistivity,[8] and we use this fact to obtain the preoperational factor, ρ^0_{mag}, which results in

$$\rho^0_{mag} = \frac{9\pi}{32}\frac{m^* N_R}{\hbar e^2}\frac{\Gamma^2}{E_F}(g-1)^2, \tag{5}$$

where m^* is the effective mass, N_R the rare earth ions density, E_F the Fermi energy, $\hbar$ is the Planck constant, and Γ defines the exchange interaction between conduction electrons of spin s and charge e at position r_e and the rare earth $4f$ ions of spin S at r_f, given by $\hat{H}_{\mathrm{exc}} = -\Gamma\,\delta(r_e - r_f)\mathrm{s}\cdot S$. The spin fluctuations have not been considered in our description.

The magnetic part of the entropy, $S(H,T)$, is given by

$$S(H,T) = \sum_i \frac{\beta E_i \exp(-\beta E_i)}{Z} + R\ln Z, \tag{6}$$

where R is the molar gas constant.

EXPERIMENTAL

The polycrystalline samples were prepared by arc melting constituent elements of purity 99.99% for aluminum and 99.9% for rare earth metals. This procedure was repeated three times in order to obtain high homogeneity samples. X-ray powder diffraction measurements were made in a Philips 1710 diffractometer with Cu $K\alpha$ radiation. The results show the presence only of the C-15 phase as confirmed by metallographic analysis. Heat capacity measurements, $C_P(H,T)$, for $H=0$ and $H=5$ T, were performed in a commercial Quantum Design PPMS 9 T. For these measurements we cut the samples in slices of approximately $3.0\times3.0\times0.2$ mm^3 with approximate mass of 10 mg. The experimental magnetic entropy change, $-\Delta S_{mag}(T)$, is obtained using the relation

$$-\Delta S_{mag}(T) = \int_0^T \frac{C_P(0,T') - C_P(H,T')}{T'}dT', \tag{7}$$

where C_P is the heat capacity measured with and without applied magnetic field, and T is the temperature of the system. In the numerator of Eq. (7) the electronic and lattice contributions can be omitted due to their weak dependence with the applied magnetic field.

The magnetization measurements as a function of temperature and magnetic field, $M(H,T)$, were performed in a commercial Quantum Design MPMS 7 T DC magnetometer with SQUID sensor. The change of magnetic entropy can be calculated also from these measurements in the region of interest using the numerical form of the Maxwell relation

$$-\Delta S_{mag}(T) = \frac{1}{2}\sum_i \left[\left(\frac{\partial M_i}{\partial T}\right)_{H_i} + \left(\frac{\partial M_{i+1}}{\partial T}\right)_{H_{i+1}}\right](H_{i+1} - H_i), \tag{8}$$

where $-\Delta S_{mag}$ is the isothermal entropy change, M_i and M_{i+1} are the experimental values of the magnetization as a function of temperature under applied magnetic field H_i and H_{i+1}, respectively, and $(H_{i+1} - H_i)$ is the isofield step.

The temperature dependence of the resistivity, $\rho(H,T)$, in zero field, as well as in presence of a 5 T dc magnetic field, was measured by the conventional four-probe method in the temperature range from 2 K up to room temperature. The samples were cut into parallelepipedal geometry with typical dimensions of $0.2\times1.0\times4.0$ mm^3. Electrical contacts were made using 60 μm diameter gold wires soldered using silver epoxy cement with a cure treatment of 200 °C/5 min. These contacts showed ohmic character with typical resistance of $\sim$100 mΩ. Resistivity measurements were done in a field cooling (FC) process in a Quantum Design PPMS 9 T system applying an ac electrical current of 1 mA and frequency of 1 Hz. No dependence in frequency was observed in these measurements, and we used 1 Hz frequency in order to be very close to a dc experiment.

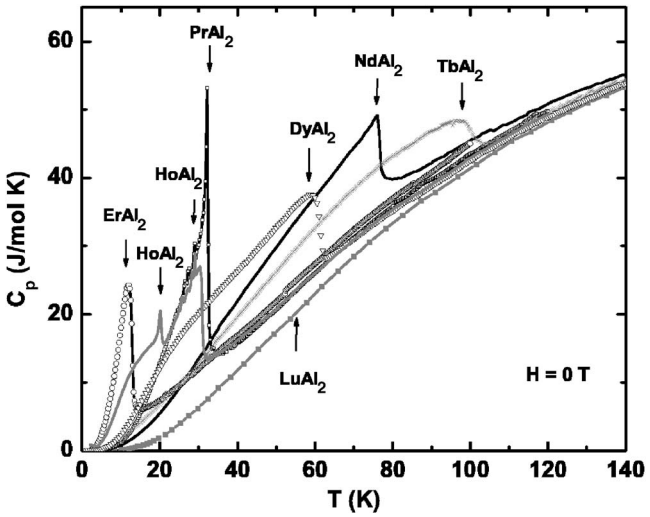

FIG. 1. Experimental heat capacities without applied magnetic field for $R\mathrm{Al}_2$ (R=Pr,Nd,Tb,Dy,Ho,Er), and LuAl_2 (Ref. 9). For the HoAl_2 compound two peaks at $T_{\mathrm{RS}}\sim 20$ K and $T_C\sim 30$ K are indicated. For the other magnetic $R\mathrm{Al}_2$ compounds the arrows show the magnetic transition temperature, T_C.

EXPERIMENTAL RESULTS

Heat capacity $C_P(H,T)$

The experimental results for heat capacity measurements with no applied magnetic field are presented in Fig. 1 for the $R\mathrm{Al}_2$ series with R=Pr,Nd,Tb,Dy,Ho,Er. In this figure it is also plotted together, as a comparison, the specific heat of the LuAl_2 compound obtained from the work of Inoue *et al.*[9] One can clearly see that a λ-type transition at the Curie temperature is obtained for these rare earth based compounds, in good agreement with the literature.[9,10] Also, it is observed that for higher temperatures the $C_P(T)$ curves closely follow the LuAl_2 behavior for which only electronic and lattice contributions are present. The magnetic contribution to the specific heat for each compound can be obtained by difference, using the nonmagnetic contribution interpolating LaAl_2 -LuAl_2 $C_P(T)$ curves. Here, we are interested in $S(0,T)-S(H,T)$ and a nonmagnetic reference is not necessary. For the HoAl_2 compound, a well defined second peak in the specific heat curve at $T_{\mathrm{SR}}\sim 20$ K is observed. At this temperature a spin reorientation transition occurs changing the easy magnetization direction from the [100] direction above T_{SR}, to [110] below T_{SR}.[11,12]

In Fig. 2 we show the $C_P(H,T)$ curves obtained for zero and for 5 T applied magnetic field for the DyAl_2 compound. One can clearly see the characteristic rapid change in the $C_P(T)$ value at the Curie temperature for $H=0$. When a magnetic field of 5 T is applied this change is not abrupt, and consequently the transition in the 5 T case is broader than in the $H=0$ case, as expected.[13] Similar behavior is observed for the whole series of compounds. From both curves obtained for each compound we calculated the isothermal magnetocaloric potential, $-\Delta S_{mag}(T)$, using Eq. (7). The results are shown in Fig. 3.

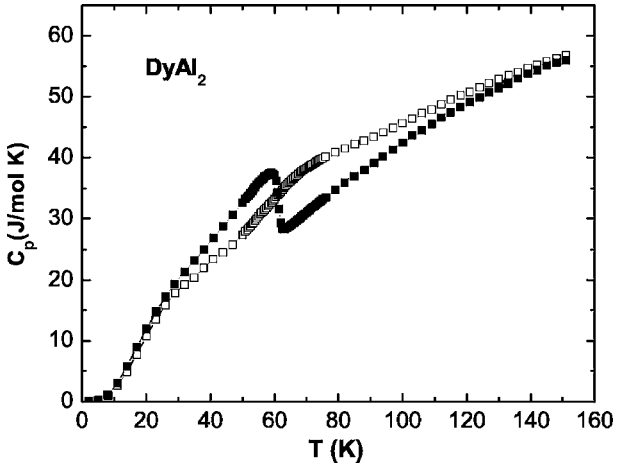

FIG. 2. Experimental heat capacities without applied magnetic field (closed squares) and at H=5 T (open squares) for DyAl_2.

Magnetization $M(H,T)$

Magnetization measurements $M(H,T)$ for some magnetic fields are shown in Fig. 4 for the TbAl_2 compound. The complete set of measurements was made with an applied magnetic field interval of 2500 Oe up to 5 T in order to calculate the magnetocaloric potential using Eq. (8). The same procedure was done for the whole series of compounds and the results for the magnetocaloric effects are in very good agreement with the ones obtained from the specific heat measurements.

Resistivity $\rho(H,T)$

The results for the electrical resistivity $\rho(H,T)$ measurements are shown in Fig. 5. We plotted the resistivity as a function of the temperature without field and for 5 T applied magnetic field for the $R\mathrm{Al}_2$ (R=Pr, Nd, Tb, Dy, Ho, and Er)

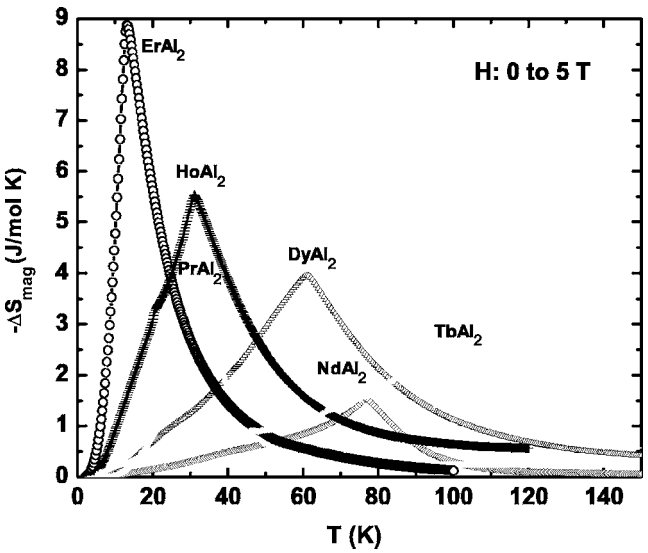

FIG. 3. $-\Delta S_{mag}$, from experimental data, as a function of temperature for the $R\mathrm{Al}_2$ series calculated for ΔH=5 T using Eq. (7), except for TbAl_2 in which case Eq. (8) was used.

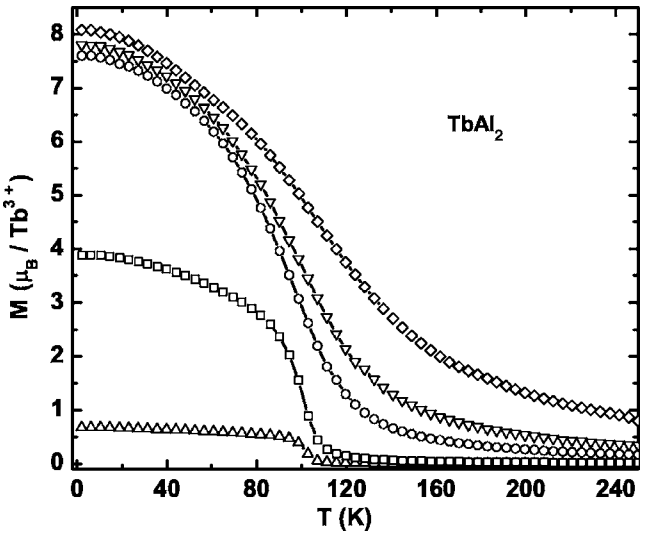

FIG. 4. Selected magnetization measurements as a function of temperature for $TbAl_2$ compound for $H=100$ Oe (△), 1 kOe (□), 1 T (○), 2 T (▽), and 5 T (◇). For $-\Delta S_{mag}$ calculation the measurements were done using a magnetic field interval of 2500 Oe.

compounds. For $H=0$ T, a kink is observed in $\rho(T)$ at the Curie transition temperature, T_C, associated with an abrupt change in the mean free path of the conduction electrons. This is related to the change in the magnetic scattering due to the transition from the ferromagnetic to the paramagnetic state. For $H=5$ T, the magnetic order extends to higher temperatures and the transition becomes smeared in temperature. The same behavior is followed by the entropy curves (not shown) which were obtained from specific heat measurements. The electric resistivity of magnetic rare earth compounds can be written[14] as the sum of the residual resistivity, ρ_R, due to imperfections and impurities, the lattice resistivity,

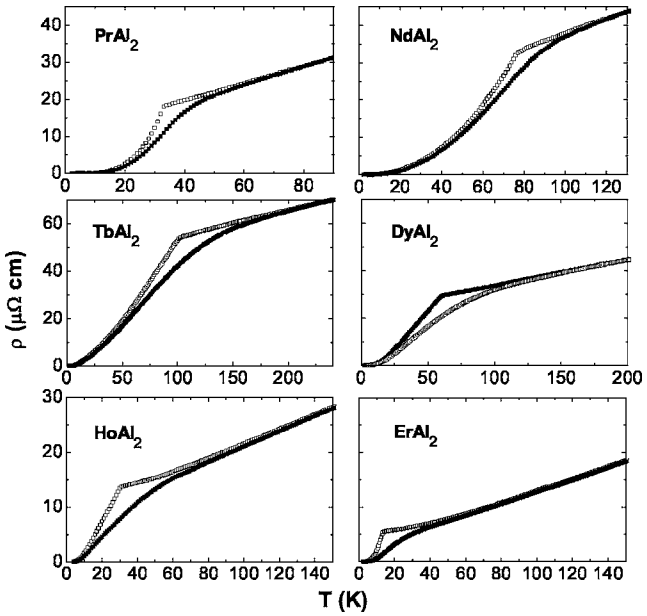

FIG. 5. Experimental resistivity as a function of temperature for $H=0$ and for $H=5$ T for RAl_2 (R=Pr, Nd, Er, Ho, Tb, and Dy) compounds after subtracting the residual resistivity.

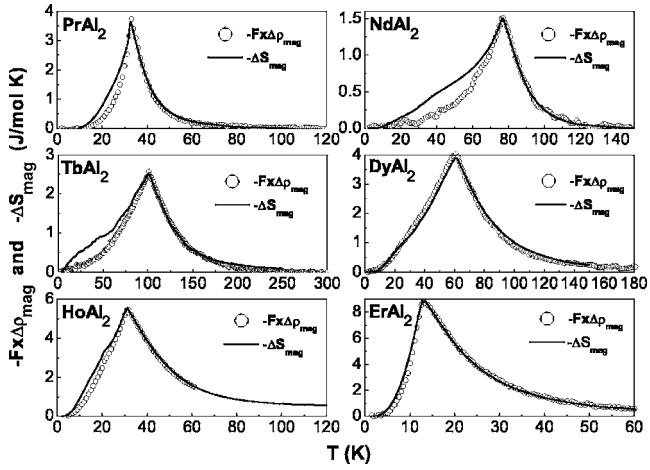

FIG. 6. Experimental $-Fx\Delta\rho_{mag}$ (circles), and $-\Delta S_{mag}$ (solid lines) vs T curves for field variation $\Delta H=5$ T for RAl_2 (R=Pr, Nd, Tb, Dy, Ho, and Er) compounds. For R=Pr, Nd, Dy, Ho, and Er, we used Eqs. (7) and (10). For $TbAl_2$ we used Eqs. (8) and (10).

ρ_{ph}, due to the phonon scattering and the magnetic resistivity, ρ_{mag}

$$\rho(H,T) = \rho_R + \rho_{ph}(T) + \rho_{mag}(H,T). \tag{9}$$

For the data in Fig. 5 we have subtracted the residual resistivity in order to compare all the samples. For temperatures far above the transitions, a linear behavior is observed, associated to the nonmagnetic phonon-electron interaction, $\rho_{ph}(T)$. The magnetic contribution, $\Delta\rho_{mag}$, is calculated directly from the resistivity measurements using Eq. (10)

$$\Delta\rho_{mag}(T) = \rho_{mag}(H,T) - \rho_{mag}(0,T) \cong \rho(H,T) - \rho(0,T)$$
$$= \Delta\rho_{total}(T), \tag{10}$$

where $\rho(H,T)$ represents the total resistivity for a specific applied magnetic field. This relation is considered valid in these compounds which present a very small magnetoelastic effect, and the mobility and concentration of carriers is essentially independent of field, so that it is a good approximation to consider that the magnetic field does not affect the phonon scattering (through the changes in the Fermi surface and in the charge carriers effects) of the electrons in the temperature interval under study. In other types of compounds, the magnetic field effects over other contributions to resistivity need to take into account to obtain $\Delta\rho_{mag}(T)$ adequately.

ANALYSIS AND DISCUSSION

Comparison of experimental $-\Delta S_{mag}$ and $-\Delta\rho_{mag}$

In Fig. 6 the temperature dependence of experimental $-\Delta S_{mag}$ is plotted together with the $-\Delta\rho_{mag}$ data for comparison. In order to match both curves for the whole range of temperatures we multiplied the resistivity by a factor F (shown in the last column in Table II). So, one can clearly see that the maxima in the $-\Delta S_{mag}$ curves coincide with the maxima in the $-F\Delta\rho_{mag}$ curves at T_C for each compound. Also, both curves are very similar to each other, but some

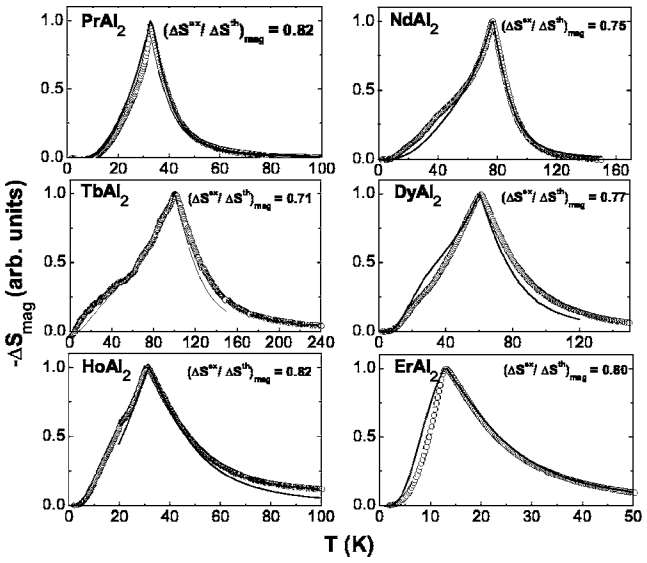

FIG. 7. Normalized $-\Delta S_{mag}$ experimental (open symbols) and theoretical (solid lines) for $\Delta H=5$ T as a function of temperature for the RAl_2 (R=Pr, Nd, Tb, Dy, Ho, and Er) compounds. Theoretical calculations were made in the easy direction. In each figure the relationship factor between experimental (ΔS^{ex}) and theoretical (ΔS^{th}) magnetic peak values are also included.

differences in their shapes are observed. For $T>T_C$, a perfect coincidence is observed between the shapes of $F\Delta\rho_{mag}$ and $-\Delta S_{mag}$ curves for the whole of the series. For $T<T_C$, near the transition, a good correlation is observed between both quantities, but at lower temperatures a T dependent factor seems necessary to better match both curves. We will further discuss this point below.

Comparison between normalized experimental and calculated $-\Delta S_{mag}$

Figure 7 shows the comparison between the normalized experimental and calculated $-\Delta S_{mag}$ curves for the series of compounds. The calculations were performed in the easy axis direction for each compound, which presents a small magnetic anisotropy. It is necessary to stress that the theoretical curves were calculated with the mean field and CEF parameters taken from the literature[2] without any fitting to our experimental data. In some cases a small correction in the molecular field parameter was performed in order to describe adequately the transition temperature. Table I shows the parameters used for the calculations and there we include the easy axis direction for the magnetization, and also the paramagnetic temperature, θ, which is considered equivalent to T_C for these ferromagnetic compounds. For $HoAl_2$ compound we show (Fig. 7) results of calculations above $T_{SR}\sim 20$ K corresponding to the [100] easy axis direction.

We see in Fig. 7 that for the Pr and Er compounds the agreement between normalized experimental and theoretical $-\Delta S_{mag}$ is very good, mainly above the transition temperature. A small deviation for temperatures higher than T_C for the Tb, Dy, and Ho cases is evident. In the ordered region, well below T_C, the experimental curves show a hump in relation to the theoretical ones, as is clear for Nd, Tb, and Dy. Theoretically in the Dy case the onset of a similar hump at higher temperatures than the experimental one was obtained, in agreement with the literature.[15] In spite of the mentioned small differences our theoretical results based in the mean field model are in good agreement with experiment for the whole of the series.

Comparison between normalized experimental and calculated $-\Delta\rho_{mag}$

The comparison between the normalized theoretical and experimental $-\Delta\rho_{mag}$ curves (Fig. 8) shows a remarkable agreement between both curves for the Pr, Dy, Ho, and Er compounds. For the Nd compound we observe small deviations for temperatures below T_C and a good agreement above this temperature. For the Tb compound there are small deviations below and above T_C. The $-\Delta S_{mag}$ calculations were based upon the assumption of magnetic isotropy. For the $-\Delta\rho_{mag}$ calculations we consider an isotropic exchange scattering [Eq. (1)]. A comparison between theory and experiment indicates that the results for $-\Delta\rho_{mag}$ are in very good agreement.

We consider that, in spite of the differences noted above, the theoretical curves obtained for the magnetocaloric effect and magnetoresistivity are good enough to be employed in a comparison between the two quantities. We suggest, from the match of these quantities, a physical procedure to obtain one curve from the other using a further experimental data, as

TABLE I. Curie temperature (θ), easy axis, mean field exchange (η), and CEF (W, X) parameters used for the calculations of $\{-\Delta S_{mag}\}$ and $\{-\Delta\rho_{mag}\}$ in the RAl_2 series. The specific heat coefficient γ (in 10^{-3} J/mol K^2) is included.

RAl_2	θ (K)	Easy axis	η (K)	W (meV)	X	γ
$PrAl_2$	33	100	9.2	−0.30	0.77	9.9
$NdAl_2$	77	100	19	0.16	−0.37	9.5
$TbAl_2$	101	111	3.2	0.020	0.91	7.7
$DyAl_2$	60	100	1.6	−0.011	0.30	7.3
$HoAl_2$	32	100	0.87	0.015	−0.34	7.0
$ErAl_2$	13	111	0.51	−0.025	−0.26	6.6

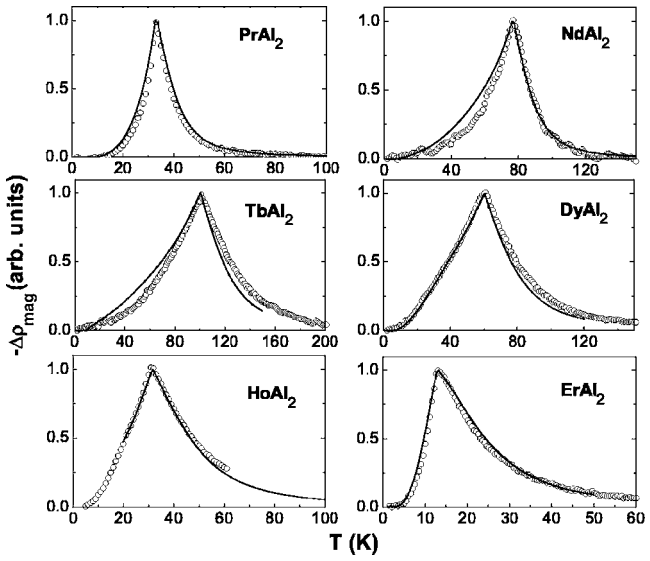

FIG. 8. Normalized $-\Delta\rho_{mag}$ experimental (open symbols) and calculated (solid lines) for $\Delta H=5$ T as a function of temperature for the RAl_2 (R=Pr, Nd, Tb, Dy, Ho, and Er) compounds.

previously done by Potter[6] for some transition metals and alloys.

Comparison between normalized theoretical $-\Delta S_{mag}$ and $-\Delta\rho_{mag}$

Figure 9 shows the comparison between the theoretical normalized results, $\{-\Delta S_{mag}\}$ and $\{-\Delta\rho_{mag}\}$, for $\Delta H=5$ T as a function of temperature for the RAl_2 (R=Pr, Nd, Tb, Dy, Ho, and Er) compounds. As noted above, for $HoAl_2$, due to the spin reorientation transition,[11,12] the calculations are shown for the temperatures above it ($T_{SR}\sim 20$ K).

For the $ErAl_2$, $HoAl_2$, and $NdAl_2$ compounds both calculated curves coincide well in the respective temperature ranges. For the $PrAl_2$ compound, a small discrepancy is observed at temperatures below T_C. For this compound one expects a strong quadrupolar interaction,[16,17] but a Hamiltonian, Eq. (2), using only the dipolar interactions gives due account of the observed features of both entropy and resistivity effects. For the $DyAl_2$ and $TbAl_2$ compounds the calculated $-\Delta S_{mag}$ curves present humps below T_C that are not observed in the calculated $-\Delta\rho_{mag}$ curves. In general, we see that the calculated MCE is very close to the calculated magnetoresistivity.

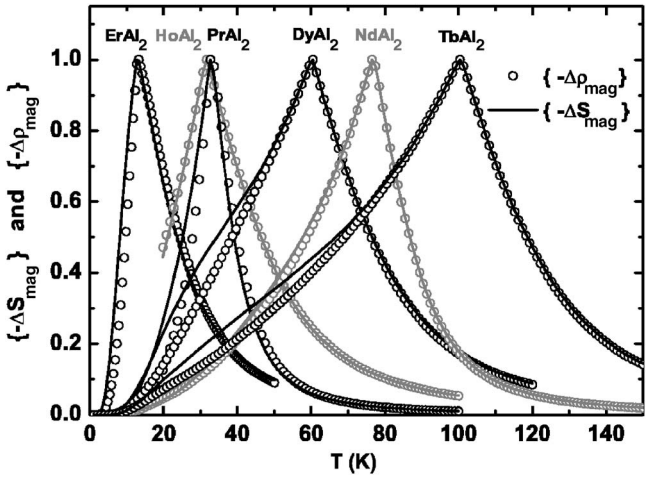

FIG. 9. Theoretical normalized results $\{-\Delta S_{mag}\}$ and $\{-\Delta\rho_{mag}\}$ for $\Delta H=5$ T as a function of temperature for the RAl_2 (R=Pr, Nd, Tb, Dy, Ho, and Er) compounds.

It is very important to try to establish theoretically a proportionality factor between the magnetoresistivity and the magnetocaloric potential.

From the well known expression for the spin disorder resistivity,[8] we obtained the factor F for the ratio of the $-\Delta S_{mag}$ and $-\Delta\rho_{mag}$ quantities given by

$$\frac{\Delta S_{mag}(T)}{\Delta\rho_{mag}(T)}=\frac{n_S}{n_\rho}\frac{32}{9\pi}\frac{\hbar e^2 E_F}{m^* N_R}\frac{1}{\Gamma^2(g-1)^2}\equiv F, \tag{11}$$

where the quantities n_s and n_ρ are defined from the relations: $-\Delta S_{mag}=n_s\{-\Delta S_{mag}\}$ and $-\Delta\rho_{mag}=\rho^0_{mag}n_\rho\{-\Delta\rho_{mag}\}$. Additionally, from the usual specific heat coefficient expression for the electronic contribution, γ, and the density of states at the Fermi energy one can obtain the following expression:

$$m^*=\frac{\hbar^2}{2}\left(\frac{48\gamma}{k_B^2 N_A a_0^3 E_F^{1/2}}\right)^{2/3} \tag{12}$$

relating the conduction electrons effective mass to the energy of the Fermi level, which in turn is related to the exchange integral by means of[8]

$$E_F=-\frac{3\pi}{4}n^2\frac{\Gamma^2}{\theta}(g-1)^2J(J+1)\Sigma_R. \tag{13}$$

In Eq. (12), N_A is the Avogadro's number, and a_0 is the lattice parameter. In Eq. (13), n is the free electron concentration, J is the total angular momentum, and Σ_R is a summation of the Ruderman-Kittel functions which for $GdAl_2$ adopt the value of -0.55×10^{-3}.[8] This value of Σ_R is used for all the compounds and we use interpolated values for γ from Ref. 15, which are shown in Table I.

Considering nine free electrons per unit formula,[8,18–20] using experimental values of Γ reported by van Daal *et al.*,[8] and the calculated values of n_S and n_ρ, one can determine the F factors using Eq. (11). Table II shows the results and the calculated values of E_F and m^*. It is interesting to note that using a simple model we reproduce well in most cases the experimental F values. For $ErAl_2$, a discrepancy due probably to a high Γ value is found, see Table II. The experimental value is reproduced using $\Gamma=11.3$ eV Å^3, and consequently, one obtains $E_F=8.7$ eV and $m^*=2.3$. Satisfactory estimates of effective masses were obtained for all the compounds.

In relation to the differences between the shapes of $-\Delta S_{mag}$ and $-\Delta\rho_{mag}$ curves (see Fig. 6) in the ordered region we can argue a temperature dependent modulating factor. An interesting study in magnetoelectronic systems[5] suggests a relation between $\Delta\rho/\Delta T$ and C_P in the transition region reinforcing our proposition ($C_P\Delta T$ and $T\Delta S$ are naturally related). In order to maintain the peak value (or the F factor),

TABLE II. Parameters used in the evaluation of the factor F in J/(mol K)/($\mu\Omega$ cm). The rare earth ions density N_R is in 10^{27} m^{-3} and Γ in eV. The effective mass m^* is in electronic mass unit (emu).

RAl_2	n_S	n_ρ	N_R	Γ	E_F (eV)	m^*	*F calc.*	*F exp.*
$PrAl_2$	4.5	8.1	15.46	27	5.1	2.6	0.51	0.53
$NdAl_2$	2.0	3.8	15.61	21	3.1	2.9	0.22	0.27
$TbAl_2$	3.6	11	16.45	14	6.7	2.1	0.28	0.23
$DyAl_2$	5.2	24	16.61	12	5.7	2.2	0.46	0.47
$HoAl_2$	6.7	35	16.75	18	15	1.5	1.2	0.95
$ErAl_2$	11	53	16.88	14	13	1.5	2.8	1.2

the relation $-F\Delta\rho_{mag}=-T\Delta S_{mag}/T_C$ is used, in the region $T<T_C$. Results are shown in Fig. 10 and one can observe a much better match between the curves for both quantities for all the compounds, except for $DyAl_2$. Once for $T>T_C$, a perfect coincidence is observed between the shapes of $-F\Delta\rho_{mag}$ and $-\Delta S_{mag}$ (Fig. 6) we propose the general relation $F\Delta\rho_{mag}(T)=(T/T_C)^m\Delta S_{mag}(T)$ to account for the observations, with $m=1$ for $T<T_C$ and $m=0$ for $T>T_C$.

Clearly, for $T<T_C$ a factor T/T_C (unity at peak) seems to take account for a better description down to lower temperatures. This is valid for all the compounds except for $DyAl_2$ for which a direct correlation ($m=0$) can be more appropriated (see Fig. 6). The T/T_C factor evidently eliminates the humps observed in the $-\Delta S_{mag}$ curves shown in Fig. 6.

Our results show that if it is possible to calculate the factor F then it is possible to obtain $-\Delta S_{mag}$ from $-\Delta\rho_{mag}$ measurements. This means that the magnetoresistivity can reliably be used as a probe for the magnetic entropy change in the RAl_2 compounds. We expect similar behavior for the RNi_2 and RNi_5 compounds because they present similar magnetic and magnetoelastic properties as the RAl_2 compounds. For the RNi_5 case it would be necessary to compare both quantities in basal and axial directions.

Recently, Rawat *et al.*[21] found a good similarity between $-\Delta S_{mag}$ and $-\Delta\rho_{mag}$ as a function of field in a large range of magnetic fields for TmCu and TmAg compounds. On the other hand, these authors reported a comparison between the total magnetoresistivity, $-\Delta\rho_{total}$, and adiabatic magnetocaloric potential, $-\Delta T_{mag}$ (generally similar in shape to $-\Delta S_{mag}$), for $PrCoSi_2$ and $Pr_{0.8}La_{0.2}Co_2Si_2$ compounds[22] showing some correlation only. From this result we stressed that to obtain adequately $-\Delta\rho_{mag}$ it can be necessary to consider a field dependence of the transport parameters in the nonmagnetic terms [Eq. (9)]. This is quite evident when one treats ferromagnetic-semiconductor manganites, for instance $La_{0.67}Ca_{0.33}MnO_3$.[23] So, to obtain a rigorous comparison between $-\Delta S_{mag}$ and $-\Delta\rho_{mag}$, the magnetic contributions to resistivity need to be adequately obtained.

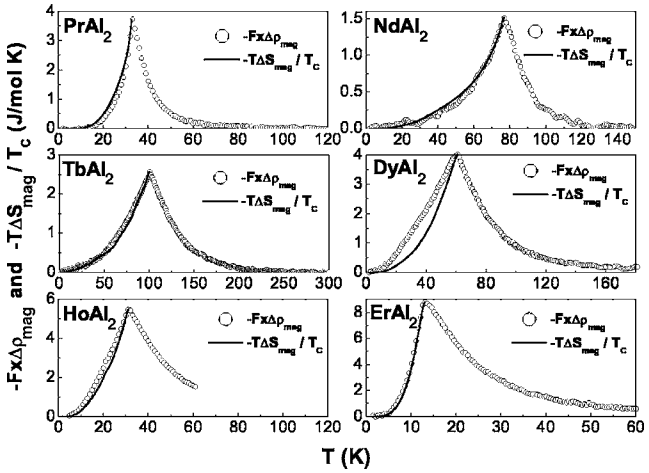

FIG. 10. Experimental $-Fx\Delta\rho_{mag}$ (circles), and $-T\Delta S_{mag}/T_C$ (solid lines) vs T curves for field variation $\Delta H=5$ T for RAl_2 (R =Pr, Nd, Tb, Dy, Ho, and Er) compounds obtained from Fig. 6.

CONCLUSIONS

We studied the close similarity between the magnetoresistivity and the magnetocaloric effect in RAl_2 intermetallic compounds and obtained for all compounds a very good description of $-\Delta S_{mag}$ and $-\Delta\rho_{mag}$ by the mean field model. Our results show that theory and experiment are in excellent agreement for both magnetocaloric and magnetoresistivity effects. Also, the results show that the magnetoresistivity as a function of temperature has the same behavior as the magnetocaloric effect in the paramagnetic region. A direct comparison of these quantities in the ordered region reveals some small deviations mainly due to the presence of a hump in the $-\Delta S_{mag}(T)$ curves for all compounds except for $DyAl_2$. Then, we suggested the relation $-F\Delta\rho_{mag}=-T\Delta S_{mag}/T_C$ in the region $T<T_C$ for an appropriate match between both quantities. Moreover, the possibility of calculation of the F factor, scaling both experimental quantities, shows that the one quantity can be used to obtain the other one. It is important to note that magnetoresistivity measurement is faster than either heat capacity or magnetization measurements typically used for $-\Delta S_{mag}(T)$ determination. In conclusion, magnetoresistivity is a reliable probe to the field induced change of magnetic entropy in the RAl_2 series. This conclusion can be extended to other rare earth based $R-X$ intermetallic compounds (excluding probably heavy fermions ones), where R is magnetic and X is nonmagnetic and, for applied magnetic fields of the order of one Tesla. For other compounds, manganites for instance, it will be necessary to be careful in order to extract adequately the magnetic contribution to resistivity. Finally, the determination of $-\Delta S_{mag}(T)$ from $-\Delta\rho_{mag}(T)$ can

be useful to study the nature of the field dependence of remnant contributions to resistivity, and can be extended to studies of barocalorimetric and colossal magnetocaloric effects which are presently very important topics.

ACKNOWLEDGMENT

The authors wish to thank Fundação de Amparo à Pesquisa do Estado de Sâo Paulo (Fapesp) for financial support.

[1] M. Ziman, *Electrons and Phonons* (Oxford University Press, London, 1972).
[2] H. G. Purwins and A. Leson, Adv. Phys. **39**, 309 (1990).
[3] V. K. Pecharsky, K. A. Gschneidner, Jr., A. O. Pecharsky, and A. M. Tishin, Phys. Rev. B **64**, 144406 (2001).
[4] H. H. Potter, Philos. Mag., Suppl. **13**, 233 (1932).
[5] S. Alexander, J. S. Helman, and I. Balberg, Phys. Rev. B **13**, 304 (1976).
[6] H. H. Potter, Proc. R. Soc. London, Ser. A **132**, 560 (1931).
[7] K. Ravishankar, M. J. Sablik, P. M. Levy, and L. F. Uffer, AIP Conf. Proc. **18**, 923 (1974).
[8] H. J. van Daal and K. H. J. Buschow, Solid State Commun. **7**, 217 (1969).
[9] T. Inoue, S. G. Sankar, R. S. Craig, W. E. Wallace, and K. A. Gschneidner, Jr., J. Phys. Chem. Solids **38**, 487 (1977).
[10] C. Deenadas, A. W. Thompson, R. S. Craig, and W. E. Wallace, J. Phys. Chem. Solids **32**, 1853 (1971).
[11] M. R. Ibarra, E. W. Lee, A. del Moral, and O. Moze, Solid State Commun. **53**, 183 (1985).
[12] M. R. Ibarra, O. Moze, P. A. Algarabel, J. I. Arnaudas, J. S. Abell, and A. del Moral, J. Phys. C **21**, 2735 (1988).
[13] R. B. Griffiths, Phys. Rev. **188**, 942 (1969).
[14] A. J. Dekker, J. Appl. Phys. **36**, 906 (1965).
[15] P. J. von Ranke, V. K. Pecharsky, and K. A. Gschneidner, Jr., Phys. Rev. B **58**, 12110 (1998).
[16] M. Christen, Solid State Commun. **36**, 571 (1980).
[17] M. J. Sablik, P. Pureur, G. Creuzet, A. Fert, and P. M. Levy, Phys. Rev. B **28**, 3890 (1983).
[18] A. Furrer and H. G. Purwins, Phys. Rev. B **16**, 2131 (1977).
[19] T. H. Tsai and D. J. Sellmyer, Phys. Rev. B **20**, 4577 (1979).
[20] H. M. Milchberg, R. R. Freeman, S. C. Davey, and R. M. More, Phys. Rev. Lett. **61**, 2364 (1988).
[21] R. Rawat and I. Das, J. Phys.: Condens. Matter **13**, L379 (2001).
[22] I. Das and R. Rawat, Solid State Commun. **115**, 207 (2000).
[23] C. M. Xiong, J. R. Sun, Y. F. Chen, B. G. Shen, J. Du, and Y. X. Li, IEEE Trans. Magn. **41**, 122 (2005).